An Analysis on the Vertical Structure of Wind Field Sounded by Doppler Sodar at Huayin

PAN, Tao; HU, Yinqiao; LIN, Peishun; MITSUTA, Yasushi

Bull. Disas. Prev. Res. Inst., Kyoto Univ., Vol. 42, Part 4, No. 370, December, 1992 115

An Analysis on the Vertical Structure of Wind Field Sounded by Doppler Sodar at Huayin

By

Tao PAN*, Yinqiao HU*, Peishun LIN**

and

Yasushi MITSUTA

(Manuscript received on Aug. 25, 1992; revised on Oct. 12, 1992; accepted on Nov. 4, 1992)

Abstract

The structure of Planetary Boundary Layer(PBL) in the HEIFE area has been preliminarily studied by Doppler Sodar in August, 1990 at Huayin station. Evolution of the PBL can be described by the Mixed Layer (ML) height increasing rapidly in daytime, and holding for a short time after the nocturnal Stable Boundary Layer(SBL) is formed in the evening. A complete process including formation, growth and disappearance of the Low-Level Jet(LLJ) was observed on August 20, 1990.

1. Introduction

Sodar has a history that goes back to 1968[1]. It has such features as easy manipulation, continuous observation and clear images of the structure of the PBL, so that it has been applied extensively to atmospheric boundary layer physics, atmospheric turbulence and air pollution, etc.. At first, it was used to measure atmorpheric phenomena such as inversion structure, thermal convection, and gravity waves in the PBL. Recent development of electronic techniques makes it also possible to make Doppler analysis of scattered signals to obtain wind velocity informations[2].

Heihe River Field Experiment, HEIFE, is a Sino-Japanese Cooperational Program on Atomsphere-Land Surface Interaction in arid areas, as the third undertaking of HAPEX in WCRP. To study the planetary boundary layer in this program, Doppler Sodar, Model HK-11, and a tethered balloon system were used in August 1990.

2. Observation Site and Data Acquisition

The site is located at Huayin station (004) in the Gobi desert in the HEIFE experimental area, and represents a typical underlying surface of Gobi desert[3]. HK-11 Doppler Sodar system[4] improved by the Electrical Instrument Factory of Peking University had been used to obtain echo intensity, three-dimensional wind-velocity

permanent affiliation: *Lanzhou Institute of Plateau Atmospheric Physics, CAS, China
**Electrical Instrument Factory, Peking University, China

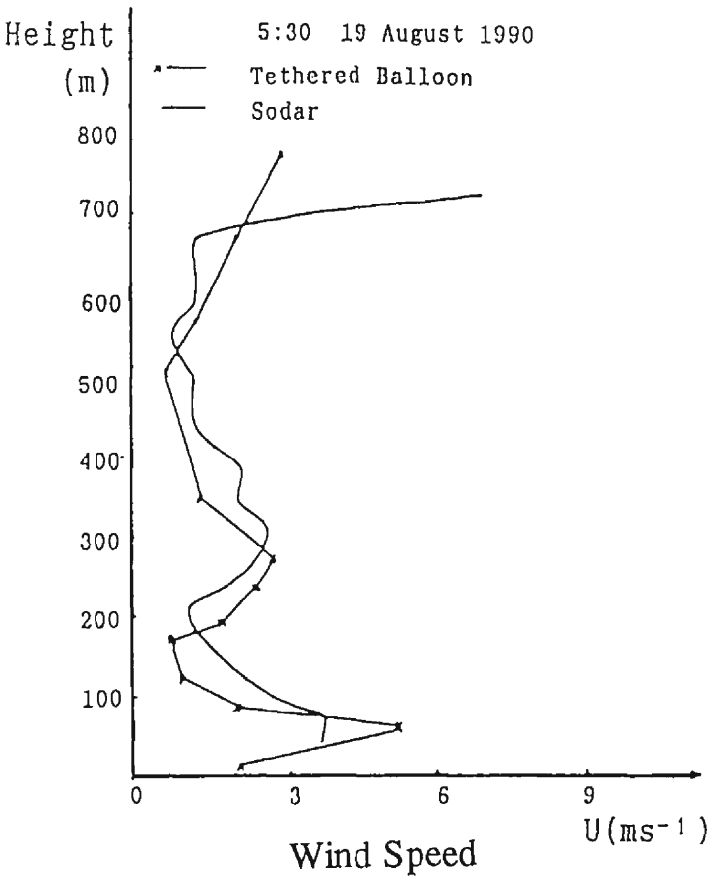

Fig. 1 The Comparison of horizontal wind speed profiles as obtained by the Doppler sodar and the tethered balloon.

and wind variances for the period from 7:00, 16th to 7:00, 24th, August in 1990. The data are averaged over every half hour. The effective detectable height above 500 meters has been attained 53.6% and that above 300 meters 91.6% of the total observation time. A tethered balloon system, a sonic anemometer and a micro-meteorological tower of the Department of Geography Sciences of Peking University, were in operation during the period. A comparison of wind speed data by Doppler sodar with that of the tethered balloon are shown in Fig. 1, and shows good agreement.

3. Determination of PBL's Height and its Evaluation Process

3.1 Basic Principle

The received echo intensity of sodar can be simplified[2] in the dry atmosphere;

$$P_r = P_0 AZ^{-2} e^{-2az} C_T^2 T^{-2} \tag{1}$$

where P_0 is the transmitted power, A constant, a an attenuation coefficient of acoustic waves through the air layer, T air temperature and C_T^2 being temperature structure function. When PBL is capped by an inversion, Wyngaard and LeMone[5] showed that within the capping inversion with a height of Z_i,

$$C_T^2 Z_i^{2/3} = f(H, \Delta\theta) \tag{2}$$

where H is the surface heat flux and $\Delta\theta$ being the temperature jumps across the interfacial region. Thus the inversion hieght can be determined from the profile of sodar's receiving echo power intensity. Normally P_r decreases exponentially with height. Taking the logarithms of both sides of Eq(1) we obtain;

$$\log P_r = \log (C_T^2 T^{-2}) - 2 \log Z - 2 aZ \log e + \text{const.} \tag{3}$$

This shows that $\log P_r$ decreases linearly with $(-2 \log Z - 2aZ \log e)$ if $C_T^2 T^{-2}$ does not change greatly with height. But $\log P_r$ deviates from the curve, if $C_T^2 T^{-2}$ changes (for example, the appearance of an inversion structure). The inversion heieght can be quantitatively determined with this relation.

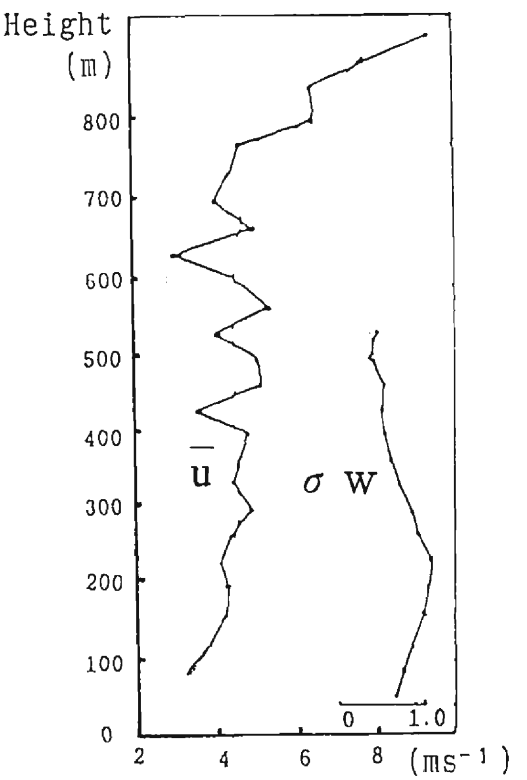

Fig. 2 The observed profiles of mean wind speed, u and standard deviation of vertical wind speed, σw at 11:30 August 20, 1990.

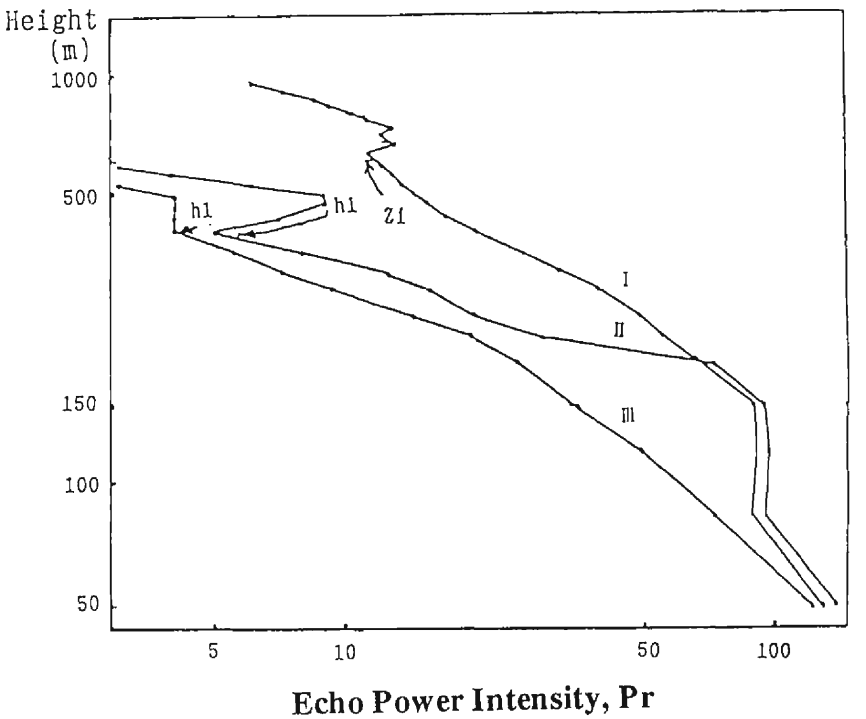

Fig. 3 The observed profiles of P_r. I at 11:30, 20st, II at 23:30, 21st and III at 20:00, 21st of August 1990.

Andre et al. (1978)[6] found that the maximum height of vertical wind speed variance σ_w, Zmax, appears at $Zi/3$, where Zi is the inversion height at ML's top. This means we can determine Zmax using the profile of σ_w and obtain $Zi=3*Z$max, when P_r profile is not clear. Fig. 2 is the observed profile of variances of vertical wind and horizontal wind speed at 11:30 on August 20th. Fig.3 shows the observed profile of P_r. The curve I is for the same time as Fig. 2, and the discontinuity of Pr is seen at about 600 m in Fig.3, which is the height of ML. The maximum of σ_w in Fig.2 is in good agreement with the above relation of $Z\max=1/3Z_i$. The horizontal wind spped, u also comes to increase rapidly in the stable layer above the inversion, which may also be used to determine the inversion height. II and III stand for the profiles of nocturnal Stable Boundary Layer. III implies a structure of multi-layer stable layer.

In order to demonstrate the effectiveness of methods to determine ML height showed above, we have selected 20 sets of data, which are sounded by Doppler sodar on clear days, to determine the ML height using the profiles of u, σ_w and P_r respectively. The three kinds of ML heights written as, $Z_i(u)$, $Z_i(\sigma_w)$ and $Z_i(P_r)$ are shown in Figs. 4a and 4b. The correlation coefficient between $Z_i(u)$ and $Z_i(P_r)$ is 0.94 and its standard deviation is 35.9 m. That between $Z_i(u)$ and $Z_i(P_r)$ is 0.89 with the standard deviation of 64.3 m. The correlation coefficients of three kinds

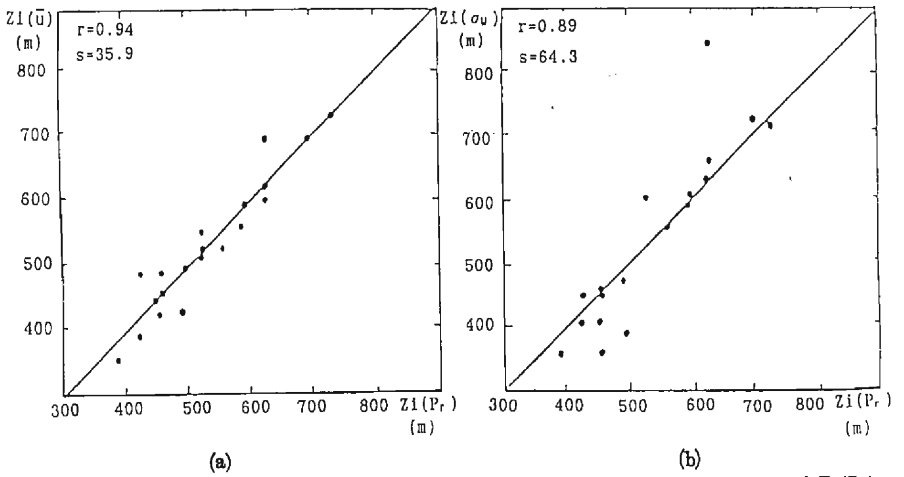

Fig. 4 Correlations between ML heights, (a) $Z_i(u)$ and $Z_i(P_r)$ and (b) $Z_i(\sigma w)$ and $Z_i(P_r)$.

of ML's heights determined by profile of u, σ_w and P_r agree considerably well. So it is practical and convenient to determine the ML's height using any of these methods.

3.2 Evolution of PBL

The evolution of PBL from 07:00 of 21st to 07:00 of 22nd, August 1990 determined by echo intensity is given in Fig. 5. This shows a complete process including the

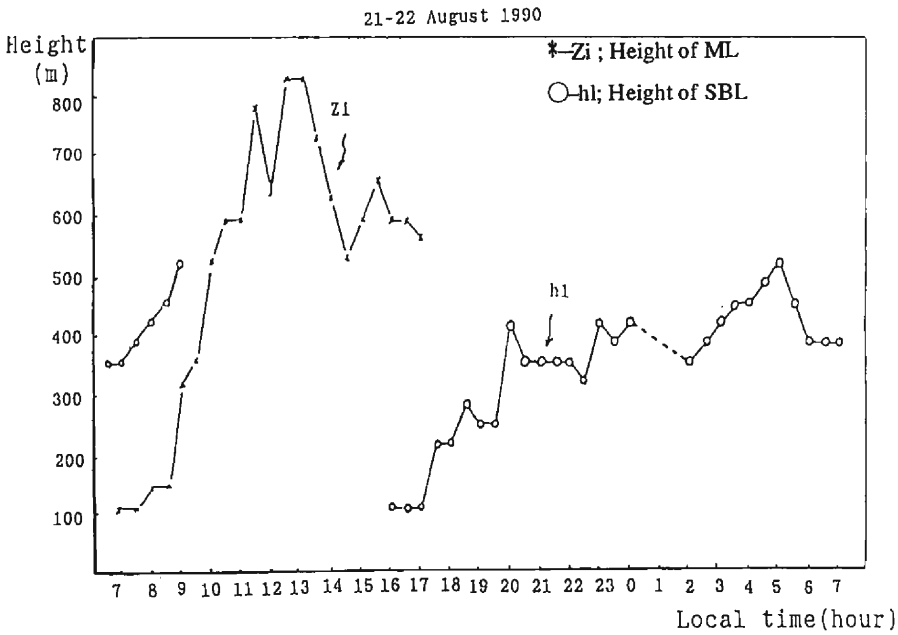

Fig. 5 Time changes of ML height(Z_i) and SBL(hl) as determined by echo intensification from 07:00, 21st to 22nd of August 1990.

formation, growth and decay of ML and SBL. This figure shows that ML starts to form at 07:00 with a depth of about 150 m above surface. It grows slowly because of the strong nocturnal stable layer capping it. ML grows rapidly after SBL disappears at 09:00, and the height of ML remains at about 650 m with fluctuations, the maximum hieght of which is 832 m. The SBL starts to form at 16:00. The ML decays completely by 17:00. Meanwhile, the height of SBL, h, increases gradually, until it fluctuates around 400 m.

It was pointed out[7] that the life cycle of ML can be divided into 4 phases; (1) Formation of a shallow ML, which slowly deepens. (2) Rapid ML growth. (3) Deep ML of nearly constant thickness. (4) Decay into turbulence. Fig. 5 shows an example of 4 phase processes measured by the sodar in the present study. During phase(1), ML's height increases slowly because of the strong nocturnal SBL capping the young ML. The top of ML depth rises at a rate of 15 m per hour. During phase(2), there is virtually no stable layer capping the ML, so that the thermals penetrate rapidly upward allowing the top of ML to rise rapidly at a rate of 450 m per hour. During phase(3), the ML depth, Zi is relatively constant during most of the afternoon. Fluctuation of the Zi may be attributed to external advaction, for instance, the subsidence induced by cold air advection from Qilian Mountain, or the entrainment at the top of ML. During phase(4), generation of convective turbulence can not be maintained against dissipation rate, because the formation of new stable stable stratification near the ground cuts off energy supply from the surface. In the absence of mechanical forcing, turbulence in the ML decays completely.

By analogy, the development of SBL can be also classified as 4 phases; (1) formation, (2) growth, (3) maturity and (4) decay. During phase (1), the ground is cooled because it emits radiation more than solar radiation recieved, so that a shallow inversion layer is formed. (2) After sunset, the inversion layer deepens with the rising of SBL as the ground becomes cooler. (3) When SBL rises to a certain height, its height stabilizes at 150 m or so. During phase (4), as the sun rises, the lower stable layer is broken down by the formation of the new ML. The upper SBL disappears as the growth of ML.

This is a whole cycle of diurnal change of PBL. From Fig. 4, it can be seen that ML grows rapidly with a rising rate of 450 m per hour more than that of SBL which rises with rate of 250 m per 3 hours because of differences in the nature of turbulence. Nevertheless, ML remains for a shorter time of only 10 hours, compared to 17 hours for SBL. The height of ML in the present case is less than that of some models[8]. This might involve special geographical environment, for example, the growth of ML is limited by advection of cooler air from the Qilian Mountain.

4. Turbulence Structure of the Mixing Layer

In the daytime, mechanical turbulence becomes unimportant compared to convection in the higher part of the boundary layer. A different type of scaling parame-

ter is required, other than the friction velocity, u_* which depends on wind speed, under those conditions. Deardorff(1970)[9] introduced a velocity scale, a convective velocity w_* defined as follows

$$w_* = \left(\frac{gHZ_i}{C_p \rho T_0}\right)^{1/3}, \tag{4}$$

where Z_i is the depth of mixing layer that represents the eddy size, H sensible heat flux in the surface layer, T_0 the surface temperature, g gravity, ρ air density and C_p being constant pressure specific heat.

With this scaling the standard deviation of vertical velocity is given by

$$\frac{\sigma_w}{w_*} = f\left(\frac{Z}{Z_i}\right). \tag{5}$$

Fig.6 shows this function in the present study. In the surface layer, $Z \leqq 0.1Z_i$, Z_i is

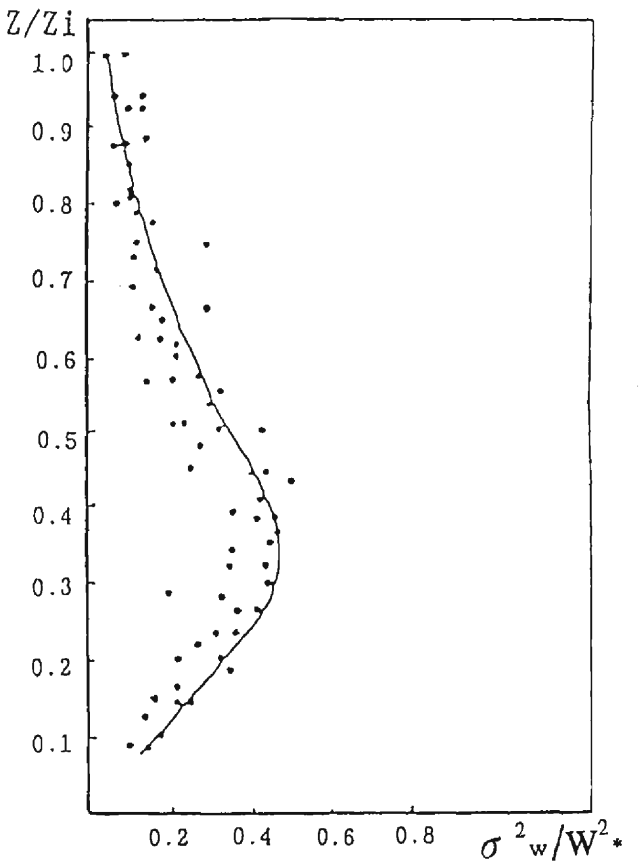

Fig. 6 The profile of normalized vertical velocity variance.

no longer important to the characteristics of σ_w. This function approaches zero at $Z/Z_i=1$, showing its maximum at about $Z/Z_i=1/3$.

5. Evolution of Low Level Jet

At the night, low level wind maximum often develops on the top of the nocturnal stable boundary layer[10]. During the observation period, a typical low level jet development was seen on the morning of August 20, 1990. Time changes of vertical distribution of horizontal wind from August 19 to August 20 are shown in Fig. 7. Wind speed in the surface layer was very weak, and was about 3 to 6 m/s at the higher level throughout the period. High level winds were higher in the daytime and lower from midnight to morning. At about 4 or 5 o'clock, lower wind speeds increases

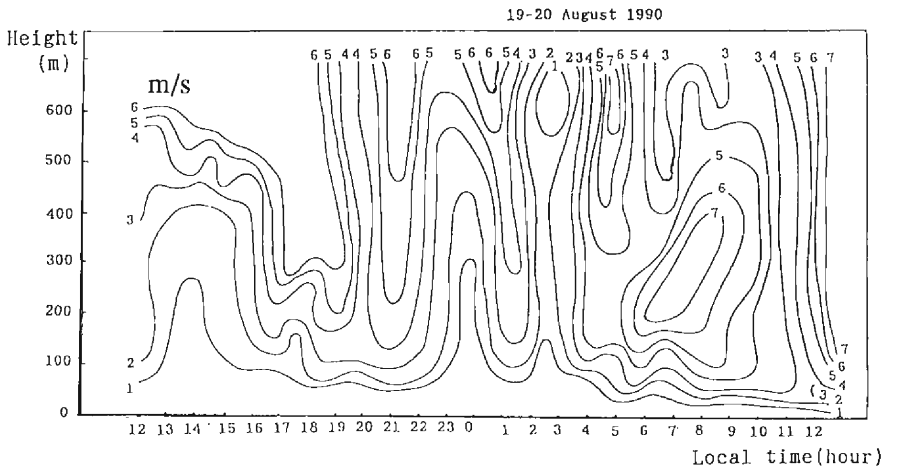

Fig. 7 Height-Time cross section of wind speed of August 19 and 20, 1990.

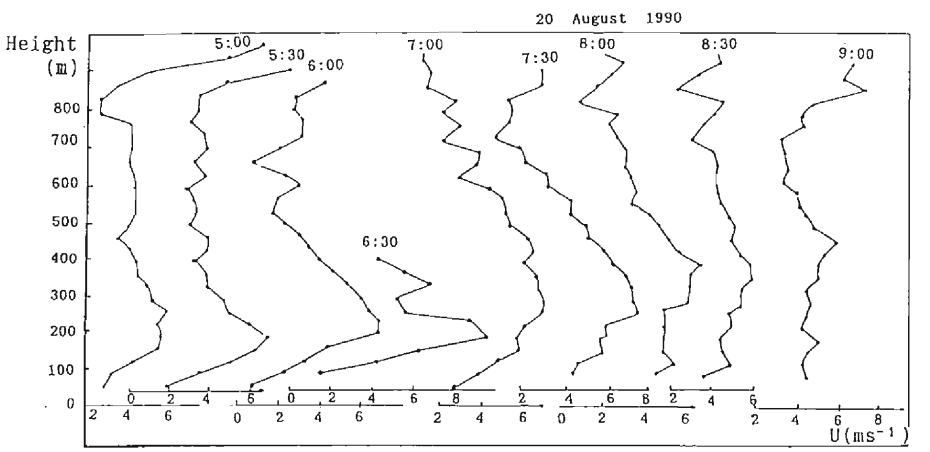

Fig. 8 Wind speed profiles on August 20, 1990.

and we could see a clear wind maximum of about 6 m/s at 200 m. The successive wind profiles after 05:00 are shown in Fig.8.

As is clear from this figure its maximum wind speed increases with time until 06:30 when it reached to about 9 m/s. After that time, the wind maximum gradually diffused and disappeared at 9 or 10 o'clock in the morning. Throughout this period, the height of the wind maximum increased gradually at first and then rapidly after its peak hour of 06:30, as shown in Fig.8.

As the related temperature profile and other meteorological parameters were not obtained for this case, the details can not be discussed further. However, the situation, that is the eastern skirt of a high mountain range, is quite similar to that of Boulder, Colorado, where a clear low level jet of almost the same features was observed by a Doppler Sodar (Kataoka et al., 1990)[11]. More detailed observations in the HEIFE will be required.

6. Conclusion

The advantages of the Doppler sodar in the observation of planetary boundary layer was clearly proved by this observation. Even in the dry atmosphere over the desert on a plateau, sound detection was possible up to about 1000 m. The phenomena observed through this observation were not so different from the results from other observations under different conditions, but they will be incorporated with other data to analyze the structure of the planetary boundary layer in this HEIFE area.

References

1) McAllister, L.G., 1975, Acoustic Sounding of Lower Troposphere, J. Atmos. Terr. Phys., 30, pp. 1429–1440.
2) Neff, W.D. and R.L. Coulter, 1986, Probing the Atmospheric Boundary Layer, ed. D. H. Lenschow, American Meteor. Soc., pp. 201–236.
3) Hu, Yinqiao, Qi Yaojin, Yang Xuanli, 1990, Preliminary Analyses about Characteristics of Microclimate and Heat Energy Budget in Hexi, Gobi(Huayin), Plateau Meteo., 9(2), pp. 113–117.
4) Yang, Y.L., X.C. Fan, L. Shusheng, X. Wubing, P. Lin and L. Weizeng, 1991, Model HK-11 Doppler Sodar - Its Principle and Application, ed. S.P. Spngal, Acoustic Remote Sensing, Tata McGraw-Hill, pp. 131–134.
5) Wyngaard, J.C. and M.A. LeMone, 1983, Behavior of Refractive Index Structure Parameter in the Entraining Convective Boundary Layer, J. Atmos. Sci., 37, pp. 1573–1585.
6) Andre, J.C., G. De Moor, P. Lacarrere, G. Therry and R. Du Vachat, 1978, Modeling the 24 hours Evolution of the Mean and Turbulent Structure of the Planetary Boundary, J. Atoms. Sci., 35, pp. 1861–1883.
7) Wilde, N.P., R.B. Stull and W. Eloranta, 1985, The LCL Zone and Cumulus Onset, J. Clim. Appl. Meteo., 24, pp. 640–657.
8) Driedonks, A.G.M. and H. Tennekes, 1984, Entrainment Effects in the Well-mixed Atmospheric Boundary Layer, Boundary Layer Meteo., 30, pp. 75–105.
9) Deardorff, J.W., 1970, Convective Velocity and Temperature Scales for the Unstable Planetary Boundary Layer, J. Atoms. Sci., 27, pp. 1211–1213.
10) Jukgen Malcher and Helmut Kraus, 1983, Low-level Jet Phenomena Described by a Integrat-

ed Dynamical PBL Model, Boundary Layre Metcor., 27, pp. 327–343.

11) Kataoka, T., M. Takehisa, Y. Ito and Y. Mitsuta, 1991, A Low Level Jet Observed by a Doppler Sodar during the International Sodar Intercomparison Experiment(ISIE), J. Meteo. Soc. Japan. 61(2), pp. 171–177.